NACA TN 4119

NATIONAL ADVISORY COMMITTEE FOR AERONAUTICS

TECHNICAL NOTE 4119

WIND-TUNNEL INVESTIGATION OF EFFECTS OF GROUND PROXIMITY AND OF SPLIT FLAPS ON THE LATERAL STABILITY DERIVATIVES OF A 60° DELTA-WING MODEL OSCILLATING IN YAW

By Byron M. Jaquet

Langley Aeronautical Laboratory
Langley Field, Va.

Washington
September 1957

NATIONAL ADVISORY COMMITTEE FOR AERONAUTICS

TECHNICAL NOTE 4119

WIND-TUNNEL INVESTIGATION OF EFFECTS OF GROUND PROXIMITY AND OF SPLIT FLAPS ON THE LATERAL STABILITY DERIVATIVES OF A 60° DELTA-WING MODEL OSCILLATING IN YAW

By Byron M. Jaquet

SUMMARY

An investigation was made in the Langley stability tunnel to determine the effects of the proximity of the ground and of split flaps on the lateral stability derivatives of a 60° delta-wing model oscillating continuously in yaw. The model was tested at ground positions between 0.30 and 1.25 mean aerodynamic chord lengths. The results of the investigation indicated that the addition of split flaps to the model produced changes in all the oscillatory stability derivatives measured, whereas the proximity of the ground produced significant changes only in the directional stability of the complete model. The proximity of the ground decreased the directional stability of the complete model with and without the split flaps and this decrease was caused by a reduction in the tail contribution as the distance between the model and the ground was decreased. With the flaps deflected and for ratios of the distance between the model and the ground to the wing mean aerodynamic chord greater than 0.50, the complete model had greater directional stability in the presence of the ground than the complete model without flaps and not in the presence of the ground.

INTRODUCTION

The effect, both theoretical and experimental, of the proximity of the ground on the longitudinal characteristics of airplanes has been known for a number of years (ref. 1) and, more recently, this effect has been the subject of investigations for swept-wing (ref. 2) and delta-wing (refs. 3 and 4) models. Essentially no information is available, however, on the effects of ground on the lateral stability characteristics of airplanes, especially for fighter types having delta wings.

The purpose of the present investigation, therefore, was to determine the effects of the proximity of the ground on the lateral stability characteristics of a 60° delta-wing model (with and without split flaps) oscillating continuously in yaw. A number of ground distances, varying from 0.30 wing mean aerodynamic chord to 1.25 wing mean aerodynamic chord, were investigated at a Mach number of 0.13 and a Reynolds number of 1.6×10^6, based on the wing mean aerodynamic chord.

SYMBOLS

The data presented herein are in the form of derivatives with respect to angular displacement, velocity, and acceleration of coefficients of rolling and yawing moments and are referred to the stability system of axes shown in figure 1. The coefficients and symbols are as follows:

C_l	rolling-moment coefficient, $\frac{\text{Rolling moment}}{q_\infty S_w b_w}$
C_n	yawing-moment coefficient, $\frac{\text{Yawing moment}}{q_\infty S_w b_w}$
b	span, ft
S	area, sq ft
c	local chord parallel to plane of symmetry, ft
$\bar{c}$	mean aerodynamic chord, $\frac{2}{S}\int_0^{b/2} c^2 dy$
q_∞	dynamic pressure, $\frac{\rho V_\infty^2}{2}$, lb/sq ft
ρ	mass density of air, slugs/cu ft
V_∞	free-stream velocity, ft/sec
α	angle of attack of reference plane, deg
β	angle of sideslip, deg or radians as noted
$\dot{\beta}$	rate of change of sideslip with time, radians/sec
ψ	angle of yaw, radians

$\dot{\psi}$ rate of change of yaw with time, radians/sec

r yawing angular velocity, $\dot{\psi}$, radians/sec

$\dot{r}$ yawing angular acceleration, $\ddot{\psi}$, radians/sec/sec

k reduced frequency parameter, $\frac{\omega b_w}{2V_\infty}$

ω circular frequency of oscillation, $2\pi f$, radians/sec

f frequency of oscillation, cps

y spanwise distance measured from and perpendicular to plane of symmetry, ft

h perpendicular distance from moment center to ground, ft

$$C_{l_\beta} = \frac{\partial C_l}{\partial \beta}$$

$$C_{n_\beta} = \frac{\partial C_n}{\partial \beta}$$

$$C_{l_r} = \frac{\partial C_l}{\partial \frac{rb_w}{2V_\infty}}$$

$$C_{n_r} = \frac{\partial C_n}{\partial \frac{rb_w}{2V_\infty}}$$

$$C_{l_{\dot{\beta}}} = \frac{\partial C_l}{\partial \frac{\dot{\beta} b_w}{2V_\infty}}$$

$$C_{n_{\dot{\beta}}} = \frac{\partial C_n}{\partial \frac{\dot{\beta} b_w}{2V_\infty}}$$

$$C_{l_{\dot{r}}} = \frac{\partial C_l}{\partial \frac{\dot{r} b^2_w}{4V_\infty^2}}$$

$$C_{n_{\dot{r}}} = \frac{\partial C_n}{\partial \frac{\dot{r} b^2_w}{4V_\infty^2}}$$

Subscripts:

t	increment in derivative due to vertical tail
w	wing
ω	denotes that parameter was measured under oscillatory conditions

MODEL AND EQUIPMENT

Model

The model used in the present investigation consisted of a 3-percent-thick 60° delta wing mounted in a midposition on a circular fuselage of fineness ratio 9. A vertical tail of aspect ratio 2.18 was mounted so that the trailing edge was coincident with the fuselage base. Split flaps (deflected 45° down at the trailing edge) having a total area of $12\frac{1}{2}$ percent of the total wing area and a constant chord of 15 percent of the mean aerodynamic chord were located on the model as indicated in figure 2. Additional characteristics of the model are given in table I. The fuselage and tail were constructed of laminated balsa with fiber-glass skin. Hardwood plugs were used where fastenings were necessary. The wing was constructed of laminated balsa with a fiber-glass skin and had two spruce spars that were perpendicular to the plane of symmetry and were glued to an aluminum-alloy mounting plate.

Ground Board

The ground board (fig. 3(a)) was constructed of plywood and had four 2- by 4-inch braces extending in the stream direction on the side away from the model (fig. 3(b)). The ground board was supported from the tunnel ceiling by four pillars (fig. 3(b)) which were adjustable

in height. In order to insure a minimum thickness of the boundary layer, which does not exist along the ground, a slot $1\frac{3}{8}$ inches wide spanned the board directly below the moment center of the model. In addition, a 2-inch-chord flap was deflected 60° to insure a pressure differential across the slot. The boundary-layer thickness was not measured. The leading-edge radius of the board was 3/4 inch.

Tunnel and Oscillation Apparatus

The tests were made in the 6- by 6-foot test section of the Langley stability tunnel (ref. 5) with the walls at zero curvature.

The equipment used to oscillate the model is shown in figure 3(c). Basically, this equipment is the same as that used for the investigation of reference 6 except for the substitution of pulleys and V-belts for the gear reduction unit. The connecting rod was pinned to an eccentric on the flywheel and transmitted a sinusoidal yawing motion to the model.

Recording of Data

The recording of data was accomplished by the equipment described in detail in reference 7. A part of this equipment was a sine-cosine resolver which was attached, through a thin shaft, to the flywheel and modified the output signals from the resistance-type strain gages used to measure the rolling and yawing moments so that the measured signals were proportional to the components of the gage signals which were in and out of phase with the motion. These signals were read visually on a highly damped direct-current meter; and the readings, when multiplied by the appropriate constants, gave the aerodynamic derivatives: $C_{l_{\beta,\omega}} + k^2 C_{l_{\dot{r},\omega}}$, $C_{n_{\beta,\omega}} + k^2 C_{n_{\dot{r},\omega}}$, $C_{l_{r,\omega}} - C_{l_{\dot{\beta},\omega}}$, and $C_{n_{r,\omega}} - C_{n_{\dot{\beta},\omega}}$. (These derivatives are obtained from equations identical to those of ref. 8.)

The effects of model inertia were, of course, eliminated by subtracting the wind-off values of these derivatives from their respective wind-on values.

TESTS AND CORRECTIONS

All tests were made in the 6- by 6-foot test section of the Langley stability tunnel (ref. 5) at a Mach number of 0.13 and a Reynolds number of 1.6×10^6, based on the wing mean aerodynamic chord.

The lateral stability derivatives were measured for the wing-body combination and the complete model (both with and without the split flaps) without ground and for the various ground distances shown in figure 3(a). The angle-of-attack range varied with the ground position (the bottom of the fuselage base was about $1\frac{1}{2}$ inches from the ground at the maximum angle) and the angle of attack was a maximum of 30° for ground positions of $0.75\bar{c}$ and greater.

All tests were made at an oscillation frequency of $1\frac{1}{4}$ cycles per second which corresponds to a reduced frequency parameter $\frac{\omega b_W}{2V_\infty}$ of 0.0821. The amplitude of yaw was $\pm 4^\circ$ for all tests. The dynamic pressure at a point $6\frac{1}{4}$ inches ahead of the moment center was measured with the ground board in each position with the model removed and it was found that the dynamic pressure varied from 24.2 pounds per square foot without ground to 30.6 pounds per square foot for the closest ground position. The data were reduced to coefficient form by using the dynamic pressure corresponding to the appropriate ground position. No jet boundary corrections were applied to the data determined during this investigation.

RESULTS AND DISCUSSION

Comparison of Oscillatory and Steady-State Derivatives

Before the effects of ground are discussed, it is of interest to determine the difference between the lateral stability derivatives of the model as determined under oscillatory conditions and steady-state conditions.

Presented in figures 4 and 5 along with the oscillatory derivatives of the present investigation are the steady-state derivatives obtained, without ground ($h/\bar{c} = \infty$), from references 9 and 10. (The model used in references 9 and 10 and the present model differed only in the material used for construction and were constructed to the same dimensions.)

In the low angle-of-attack range there is little difference between the steady-state derivative C_{l_β} and the oscillatory derivative $C_{l_{\beta,\omega}} + k^2 C_{l_{\dot{r},\omega}}$ (fig. 4(a)) for the model with and without the tail. For angles of attack above 5° the oscillatory derivative becomes progressively larger as the angle of attack is increased. A difference between the steady-state derivative C_{n_β} and the oscillatory derivative $C_{n_{\beta,\omega}} + k^2 C_{n_{\dot{r},\omega}}$ (fig. 4(c)) occurs only at angles of attack greater than

about 20° with the tail off, the values of C_{n_β} being more negative (unstable). These differences in derivatives measured under steady and oscillatory conditions may be attributable to frequency effects since the amplitude for which the derivatives were measured was approximately the same for both cases (±4° for the oscillatory case and ±5° for the steady-state case). Similar results have been noted for swept and delta wings in references 6 and 8.

For the complete model (fig. 4(c)), the oscillatory value of the directional stability is about 26 percent greater at $\alpha = 0°$ than the steady-state value, the increment being more or less constant through the angle-of-attack range investigated. This increase in directional stability is the result of an increase in the tail contribution (fig. 6(a)) under the oscillatory conditions. Results similar to these have been previously shown in reference 11 for a swept-wing model and also show an increase in the tail contribution with an increase in the frequency of oscillation.

It has been shown in references 6 and 8 that, at relatively moderate angles of attack in a yawing oscillation about a vertical axis, the oscillatory derivatives $C_{l_{r,\omega}} - C_{l_{\dot{\beta},\omega}}$ and $C_{n_{r,\omega}} - C_{n_{\dot{\beta},\omega}}$ are considerably larger than the steady-state derivatives C_{l_r} and C_{n_r}, the difference being attributed to the large magnitude of the $\dot{\beta}$ terms.

This is true in the present investigation where the steady-state C_{l_r} and oscillatory $C_{l_{r,\omega}} - C_{l_{\dot{\beta},\omega}}$ cross derivatives differ greatly at angles of attack above about 10° (fig. 5(a)), the oscillatory derivatives being much larger in magnitude, and this is true with the tail on or off. A similar situation exists for the steady-state C_{n_r} and oscillatory $C_{n_{r,\omega}} - C_{n_{\dot{\beta},\omega}}$ damping derivatives (fig. 5(c)), the greatest damping being obtained under oscillatory conditions with the tail on or off. In reference 8, these large oscillatory derivatives are attributable to an incremental moment (rolling or yawing) which is produced by flow separation and which lags the yawing motion by a time interval that is about constant.

Effect of Ground

In order to determine the effects of the proximity of the ground on the lateral oscillatory stability derivatives of the model, tests were made in the presence of the ground board at distances varying from $0.30\bar{c}_w$ to $1.25\bar{c}_w$ between the model and the ground and without ground, which actually corresponded to a distance between the model and the ceiling of $1.72\bar{c}_w$.

The results of these tests indicate that, except for the directional stability derivative of the complete model (figs. 4(c) and 4(d)), the effects of the proximity of the ground on the lateral oscillatory derivatives are relatively small and inconsistent. (See figs. 4 and 5.) The directional stability parameter $C_{n_{\beta,\omega}} + k^2 C_{n_{\dot{r},\omega}}$ of the complete model without and with split flaps is generally reduced as the distance between the ground and the model is decreased, the largest reductions occurring at moderate and high angles of attack. The changes in the oscillatory directional stability of the complete model (with and without flaps) are the result of a decrease in the tail contribution due to the proximity of the ground. (See fig. 6.) The effects of the proximity of the ground on the tail contribution to the out-of-phase lateral oscillatory derivatives are generally negligible. (See fig. 7.)

Effect of Split Flaps

Since it has been previously noted that the ground effects on the lateral oscillatory derivatives were, in general, small, the following discussion of flap effects will generally be confined to the data obtained without ground. For convenience, these data are replotted in figures 8 and 9.

The addition of split flaps (deflection 45°; trailing edge down) to the model produced a negative increment in $C_{l_{\beta,\omega}} + k^2 C_{l_{\dot{r},\omega}}$ at angles of attack below about 16° for the tail-off configuration and below about 20° for the complete model (fig. 8(a)); the increment was about constant for angles of attack between 0° and 10°. In the high angle-of-attack range the increment due to the flaps was positive or negative depending on the angle of attack. The negative increment in $C_{l_{\beta,\omega}} + k^2 C_{l_{\dot{r},\omega}}$ at low angles of attack might be expected on the basis of the steady-state results in the investigation of a 45° swept wing of aspect ratio 4 reported in reference 12. It was also shown therein that for short-span inboard flaps the increment was of opposite sign in the low angle-of-attack range.

With the tail off, the directional instability of the model was increased (fig. 8(b)) by the addition of the split flaps whereas with the tail on the directional stability was increased when the flaps were added to the model. This latter effect with the complete model tends to counteract the decrease in directional stability caused by the proximity of the ground (fig. 4(c)) so that with the flaps deflected the complete model in the presence of the ground for ground distances greater than $h/\bar{c} = 0.50$ has more directional stability than when the flaps are removed (fig. 4(d)) and the model is not in the presence of the ground ($h/\bar{c} = \infty$).

Except for angles of attack greater than 26°, the cross derivative $C_{l_{r,\omega}} - C_{l_{\dot{\beta},\omega}}$ (fig. 9(a)) became more positive with the tail on or off when the flaps were added to the model. The model possibly experienced an outboard movement of the lateral center of pressure at angles of attack near 10°; this movement would result in an increase in the value of $C_{l_{r,\omega}} - C_{l_{\dot{\beta},\omega}}$. On the basis of a steady-state investigation (ref. 13) of a 45° sweptback wing of aspect ratio 2.61, the increment in the cross derivative due to flaps may be positive or negative depending on the flap span.

The addition of the flaps to the model, with or without the tail, generally resulted in an increase in the damping derivatives $C_{n_{r,\omega}} - C_{n_{\dot{\beta},\omega}}$ (fig. 9(b)). This result was also indicated for the model used in the investigation of steady-state damping in yaw C_{n_r} in reference 13 for a flap span similar to that of the present model.

In general, it can be said that the addition of split flaps to the model produced changes in all the oscillatory derivatives measured, whereas the proximity of the ground to the model only produced significant changes in the directional stability of the complete model.

CONCLUSIONS

An investigation made at low speed, in the Langley stability tunnel, to determine the effects of the proximity of the ground and of split flaps on the lateral stability derivatives of a 60° delta-wing model oscillating continuously in yaw has indicated the following conclusions:

1. The addition of split flaps to the model produced changes in all the oscillatory derivatives measured whereas the proximity of the ground produced significant changes only in the directional stability of the complete model.

2. The proximity of the ground decreased the directional stability of the complete model with and without the split flaps, and this decrease was caused by a reduction of the tail contribution as the distance between the model and the ground decreased.

3. With the flaps deflected, and for ratios of the distance between the model and the ground to the wing mean aerodynamic chord greater than 0.50, the complete model had greater directional stability in the presence

of the ground than the complete model without flaps and not in the presence of the ground.

Langley Aeronautical Laboratory,
National Advisory Committee for Aeronautics,
Langley Field, Va., May 16, 1957.

REFERENCES

1. Pistolesi, E.: Ground Effect - Theory and Practice. NACA TM 828, 1937.

2. Furlong, G. Chester, and Bollech, Thomas V.: Effect of Ground Interference on the Aerodynamic and Flow Characteristics of a 42° Swept-back Wing at Reynolds Numbers Up to 6.8×10^6. NACA Rep. 1218, 1955. (Supersedes NACA RM L8G22 and NACA TN 2487.)

3. Scallion, William I.: The Effect of Ground on the Low-Speed Aerodynamic, Control, and Control Hinge-Moment Characteristics of a Delta-Wing—Fuselage Model with Trailing-Edge Controls. NACA RM L54H03, 1954.

4. Buell, Donald A., and Tinling, Bruce E.: Ground Effects on the Longitudinal Characteristics of Two Models With Wings Having Low Aspect Ratio and Pointed Tips. NACA RM A55E04, 1955.

5. Bird, John D., Jaquet, Byron M., and Cowan, John W.: Effect of Fuselage and Tail Surfaces on Low-Speed Yawing Characteristics of a Swept-Wing Model As Determined in Curved-Flow Test Section of Langley Stability Tunnel. NACA TN 2483, 1951. (Supersedes NACA RM L8G13.)

6. Fisher, Lewis R.: Experimental Determination of the Effects of Frequency and Amplitude on the Lateral Stability Derivatives for a Delta, a Swept, and an Unswept Wing Oscillating in Yaw. NACA RM L56A19, 1956.

7. Queijo, M. J., Fletcher, Herman S., Marple, C. G., and Hughes, F. M.: Preliminary Measurements of the Aerodynamic Yawing Derivatives of a Triangular, a Swept, and an Unswept Wing Performing Pure Yawing Oscillations, With a Description of the Instrumentation Employed. NACA RM L55L14, 1956.

8. Campbell, John P., Johnson, Joseph L., Jr., and Hewes, Donald E.: Low-Speed Study of the Effect of Frequency on the Stability Derivatives of Wings Oscillating in Yaw With Particular Reference to High Angle-of-Attack Conditions. NACA RM L55H05, 1955.

9. Goodman, Alex, and Thomas, David F., Jr.: Effects of Wing Position and Fuselage Size on the Low-Speed Static and Rolling Stability Characteristics of a Delta-Wing Model. NACA Rep. 1224, 1955. (Supersedes NACA TN 3063.)

10. Jaquet, Byron M., and Fletcher, Herman S.: Experimental Steady-State Yawing Derivatives of a 60° Delta-Wing Model As Affected by Changes in Vertical Position of the Wing and in Ratio of Fuselage Diameter to Wing Span. NACA TN 3843, 1956.

11. Fisher, Lewis R., and Fletcher, Herman S.: Effect of Lag of Sidewash on the Vertical-Tail Contribution to Oscillatory Damping in Yaw of Airplane Models. NACA TN 3356, 1955.

12. Lichtenstein, Jacob H., and Williams, James L.: Effect of High-Lift Devices on the Static-Lateral-Stability Derivatives of a 45° Sweptback Wing of Aspect Ratio 4.0 and Taper Ratio 0.6 in Combination With a Body. NACA TN 2819, 1952.

13. Lichtenstein, Jacob H.: Effect of High-Lift Devices on the Low-Speed Static Lateral and Yawing Stability Characteristics of an Untapered 45° Sweptback Wing. NACA TN 2689, 1952. (Supersedes NACA RM L8G20.)

TABLE I.- MODEL DETAILS

Wing:	
Aspect ratio	2.31
Taper ratio	0
Span, ft	3.042
Area, sq ft	4.005
Root chord, ft	2.635
Mean aerodynamic chord, ft	1.758
Quarter-chord sweep angle, deg	52.2
Dihedral angle, deg	0
Geometric twist, deg	0
Incidence, deg	0
Airfoil section parallel to plane of symmetry	NACA 65A003
Split flaps (dimensions of one):	
Area, sq ft	0.251
Span, ft	0.954
Inboard edge location, percent wing semispan	0.164
Chord, percent wing mean aerodynamic chord	15
Deflection with respect to wing chord plane and parallel to plane of symmetry, deg	0, 45
Vertical tail (to reference line):	
Aspect ratio	2.18
Taper ratio	0
Span, ft	1.123
Area, sq ft	0.579
Root chord, ft	1.029
Mean aerodynamic chord, ft	0.687
Quarter-chord sweep angle, deg	34.5
Airfoil section parallel to root chord	NACA 65006
Tail length from wing chord of mean aerodynamic quarter chord to tail chord of mean aerodynamic quarter chord, ft	1.738
Ratio of tail area to wing area	0.144
Tail volume	0.082
Fuselage:	
Length, ft	2.700
Fineness ratio	9.00
Cross-section shape	Circular

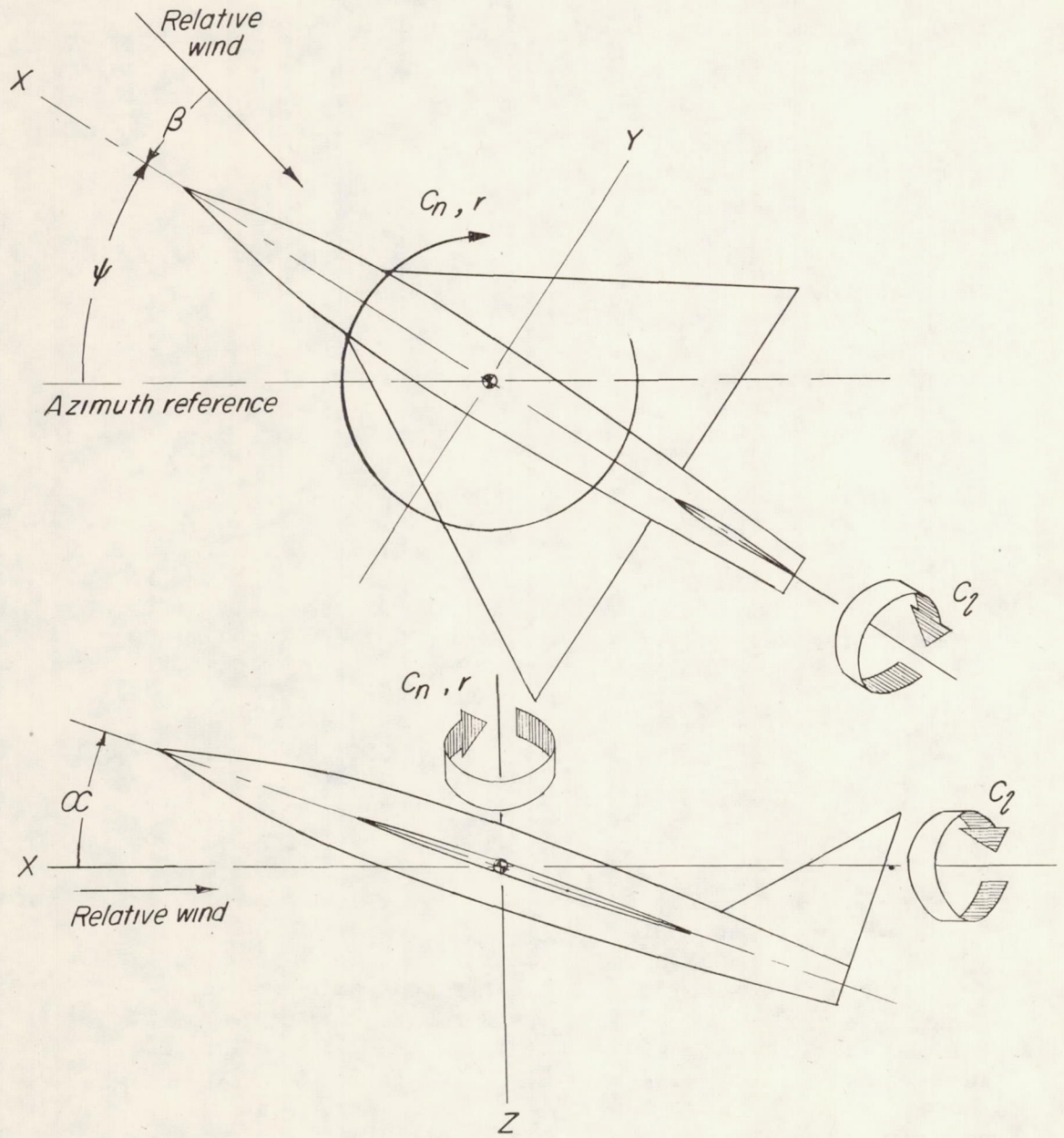

Figure 1.- Stability system of axes. Arrows indicate positive coefficients, velocities, and displacements.

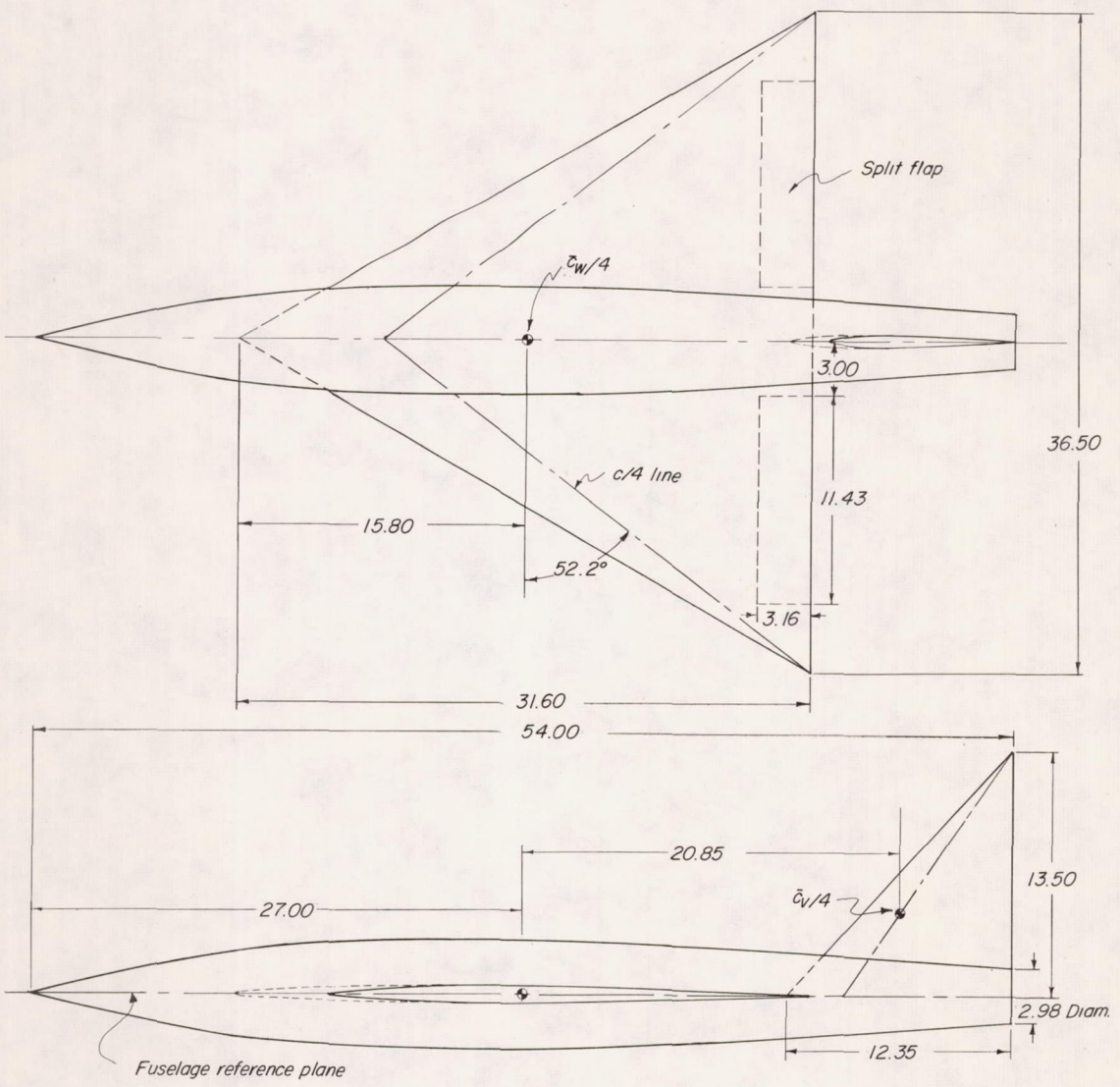

Figure 2.- Model details. Dimensions are in inches.

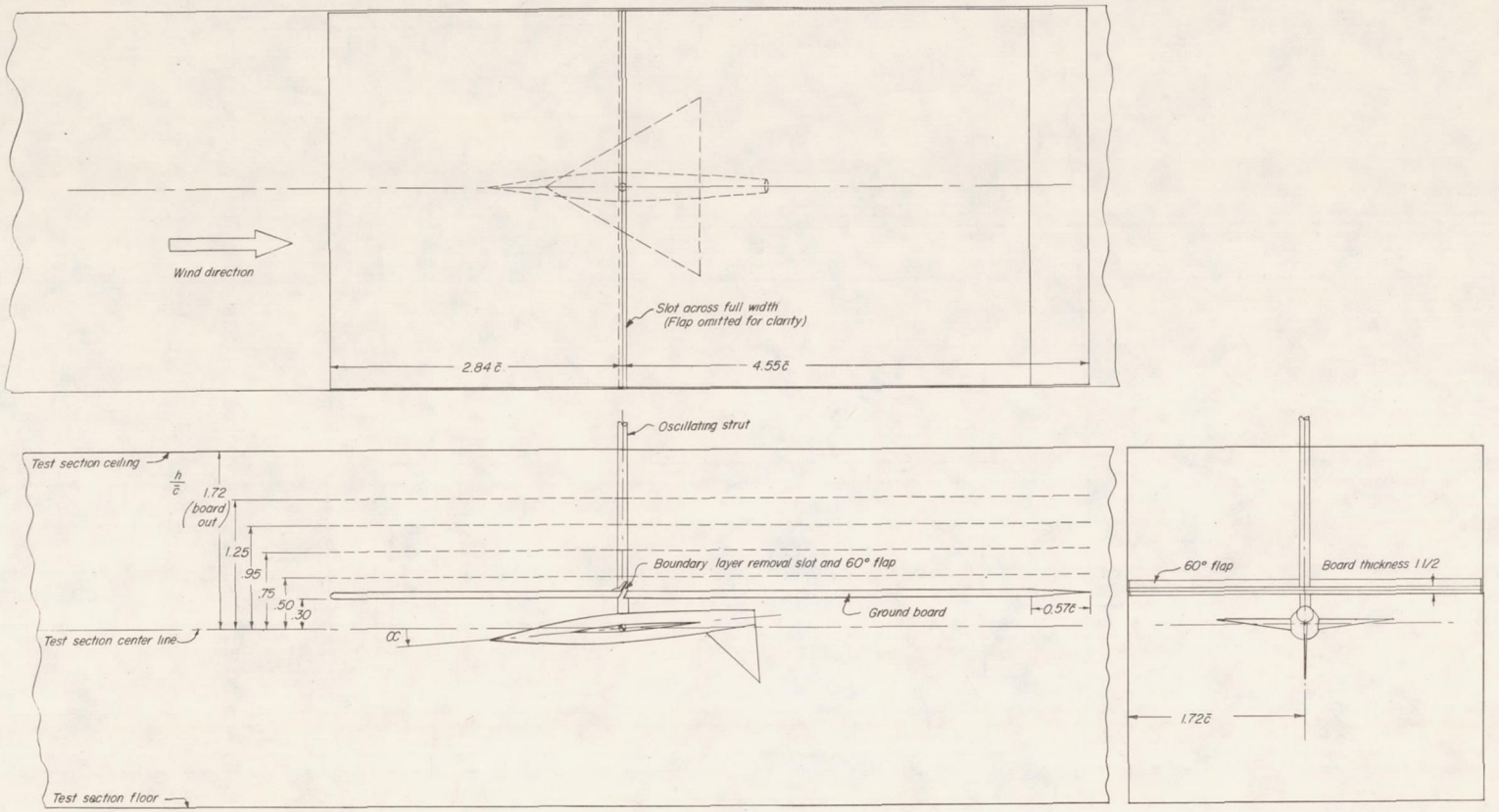

(a) Ground board installation.

Figure 3.- Test apparatus. Positive angle of attack shown.

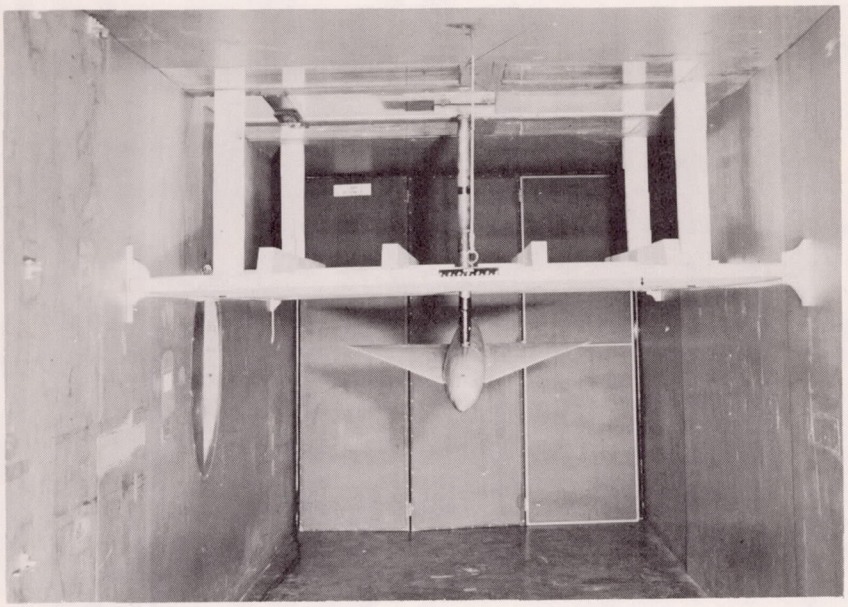

L-95671

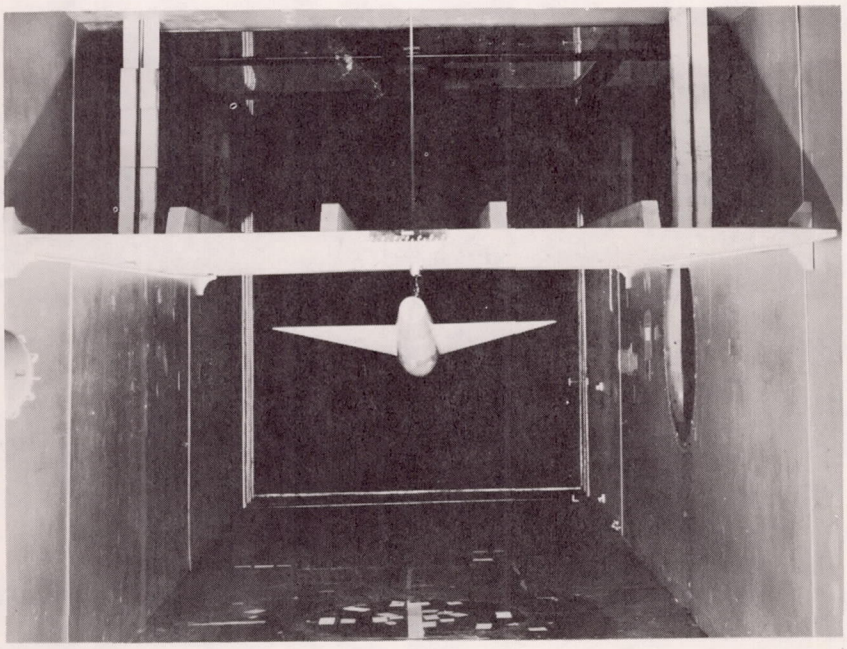

(b) Model in tunnel. L-95670

Figure 3.- Continued.

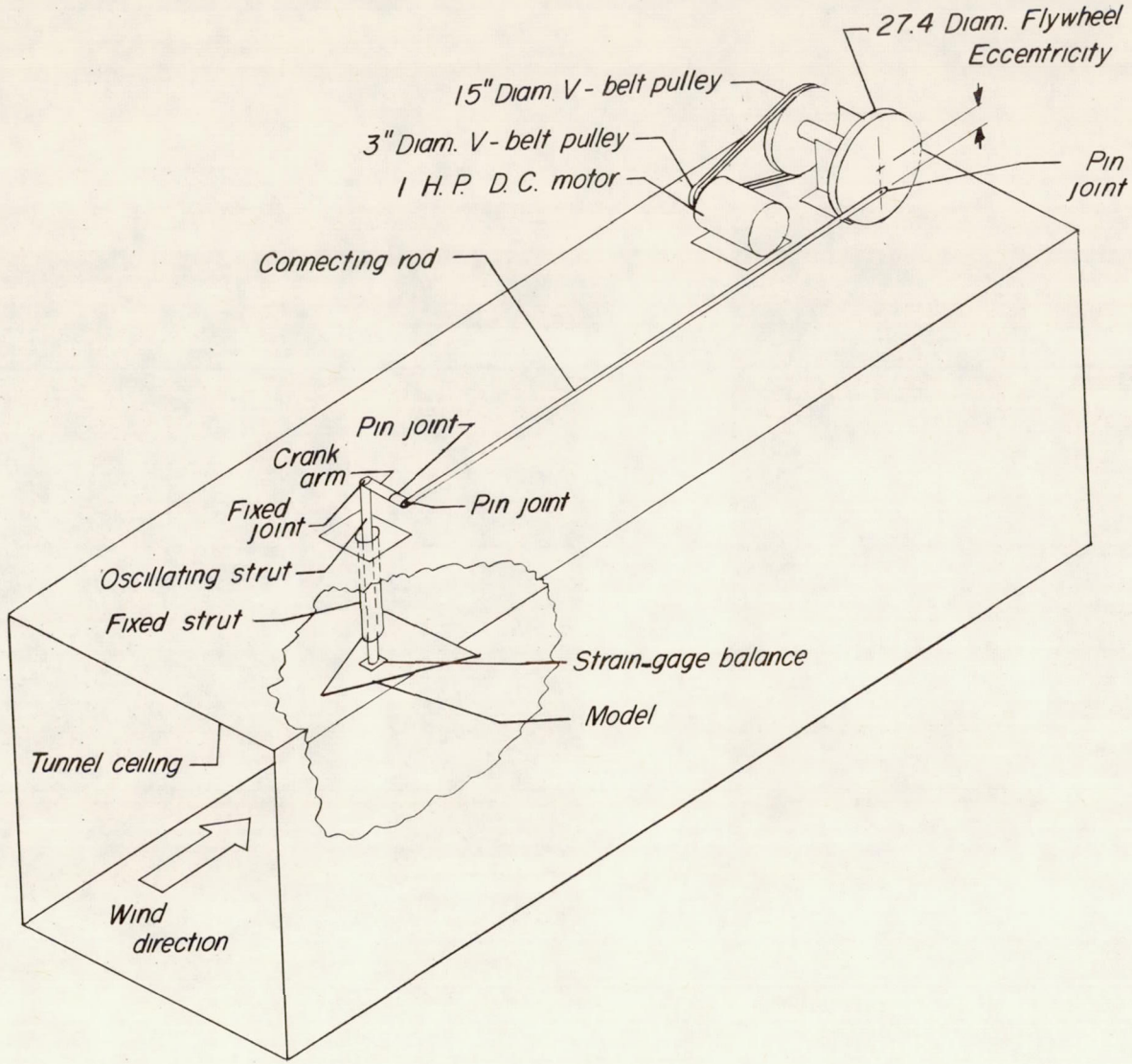

(c) Oscillation equipment.

Figure 3.- Concluded.

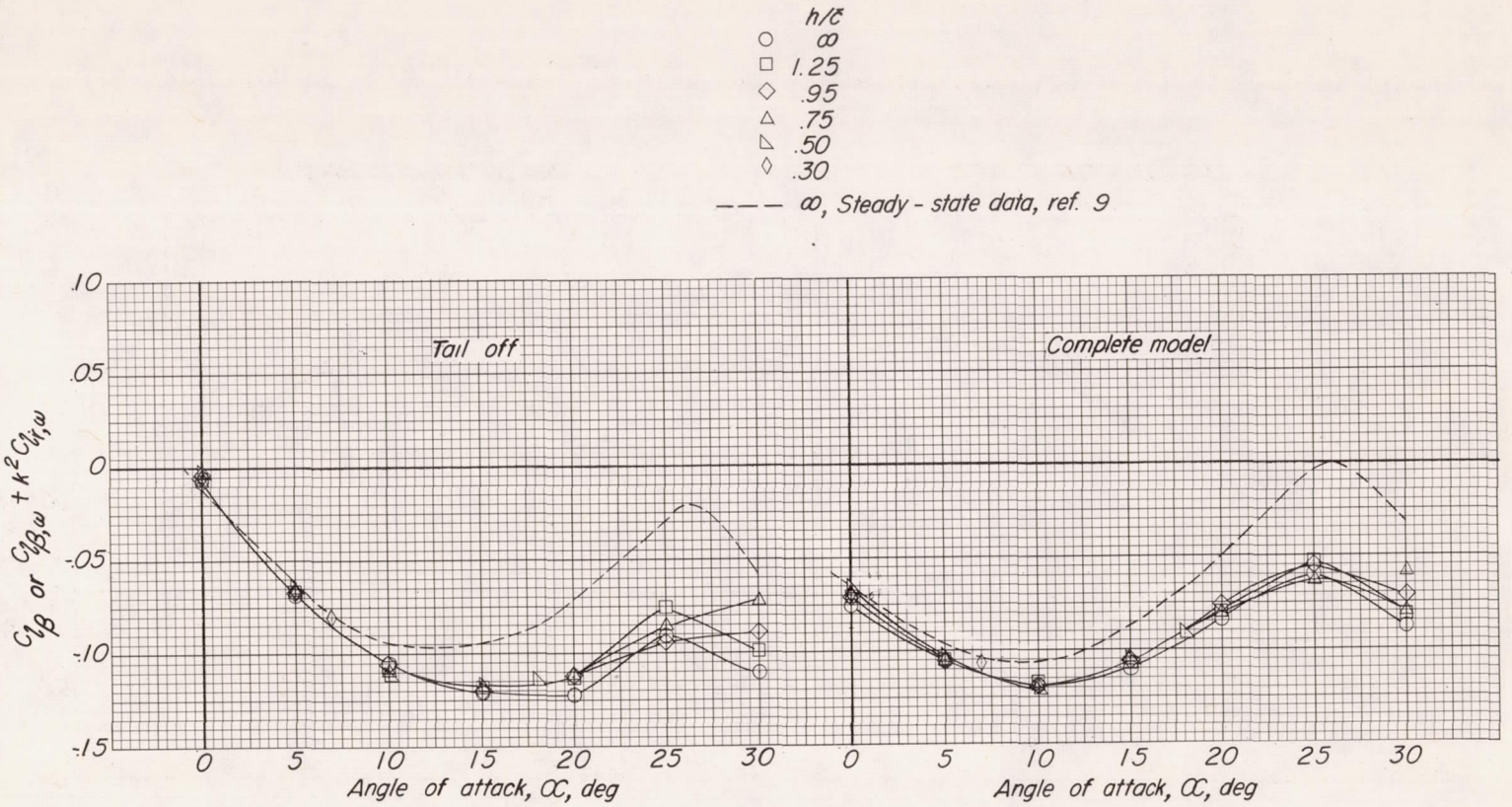

(a) Variation of C_{l_β} and $C_{l_{\beta,\omega}} + k^2 C_{l_{\dot{r},\omega}}$ with angle of attack for the model without split flaps.

Figure 4.- Effect of ground on the in-phase lateral oscillatory stability derivatives of a 60° delta-wing model with and without a vertical tail.

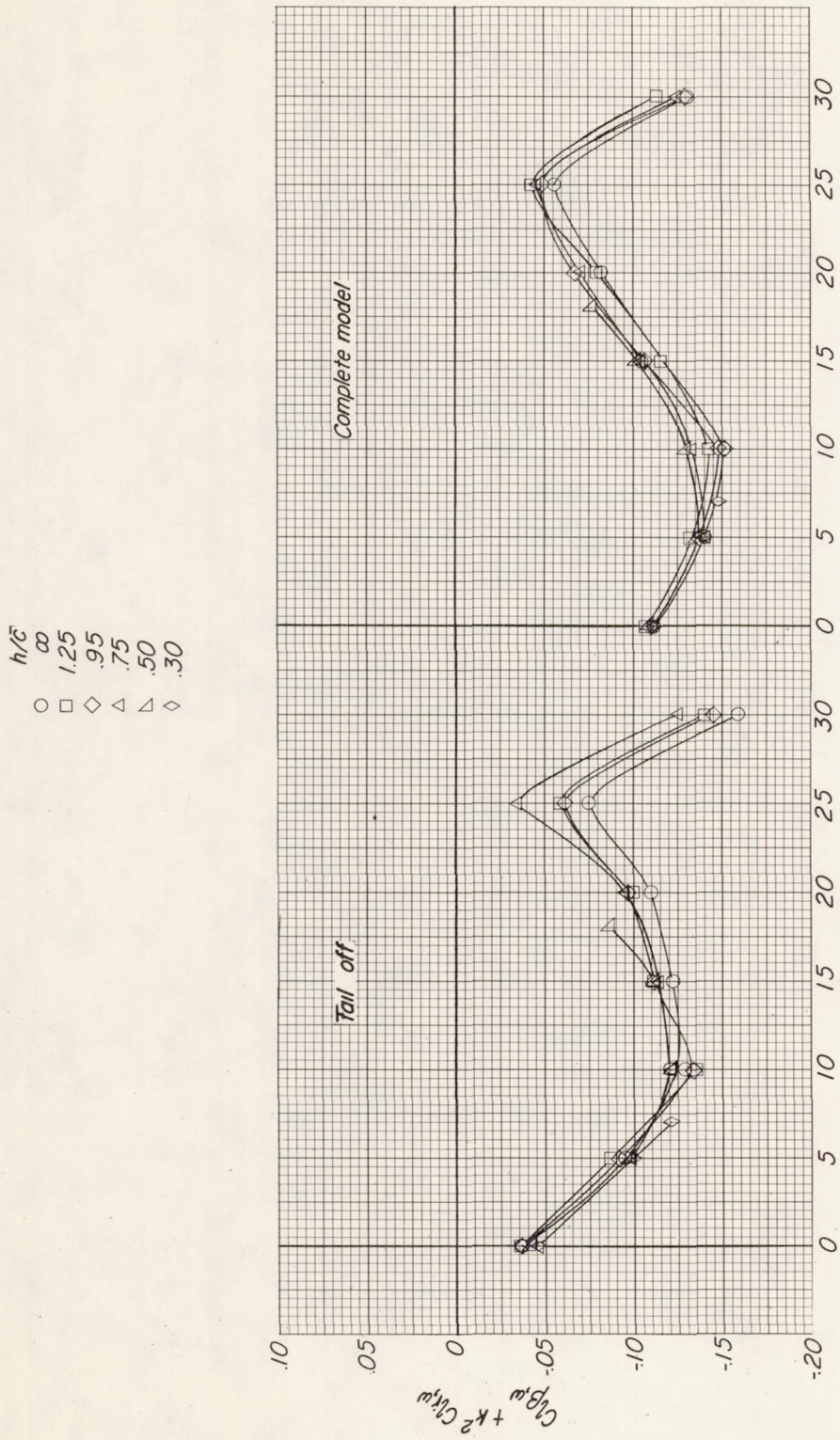

(b) Variation of $C_{l_{\beta,\omega}} + k^2 C_{l_{\dot{r}},\omega}$ with angle of attack for the model with split flaps.

Figure 4.- Continued.

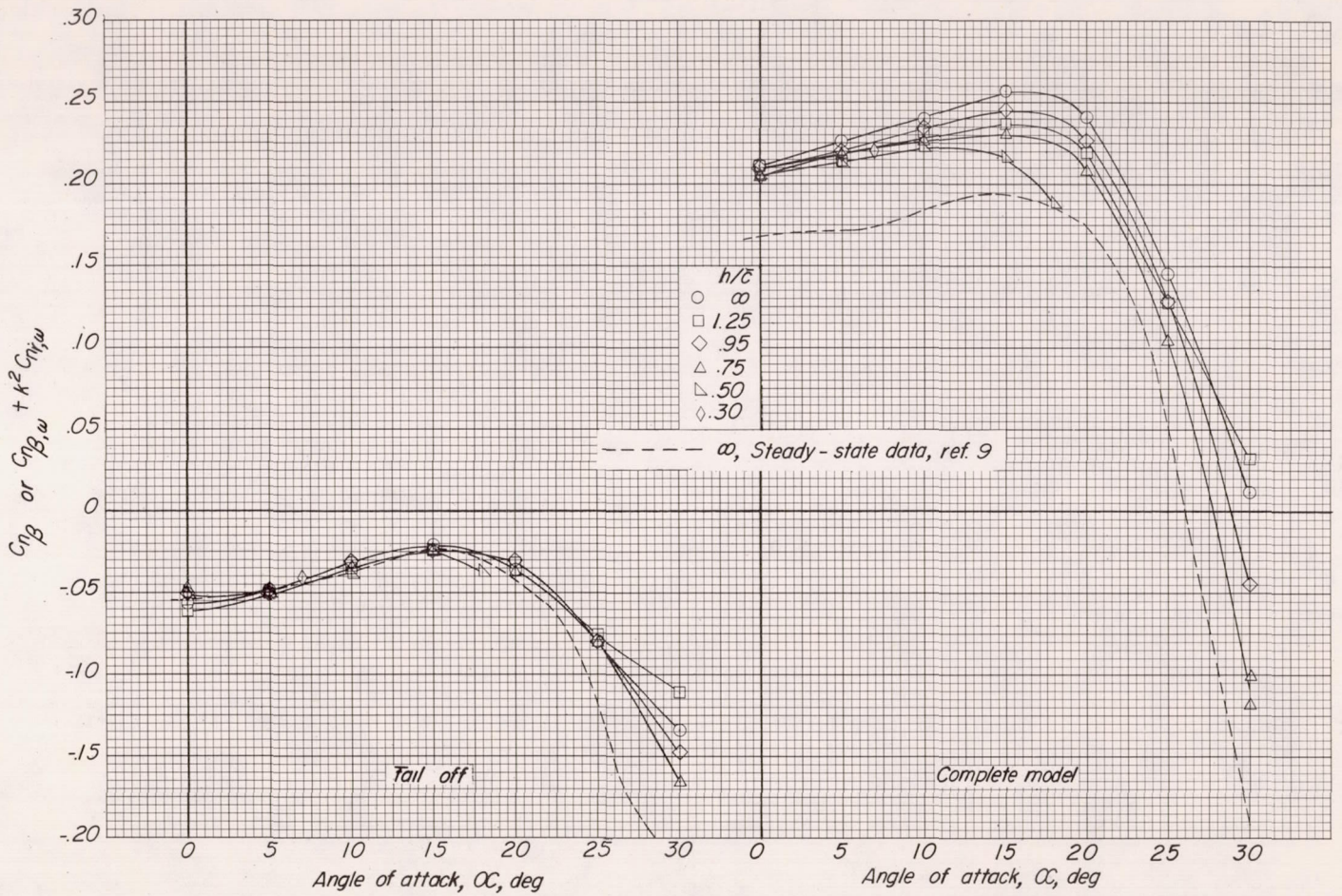

(c) Variation of C_{n_β} and $C_{n_{\beta,\omega}} + k^2 C_{n_{\dot{r},\omega}}$ with angle of attack for the model without split flaps.

Figure 4.- Continued.

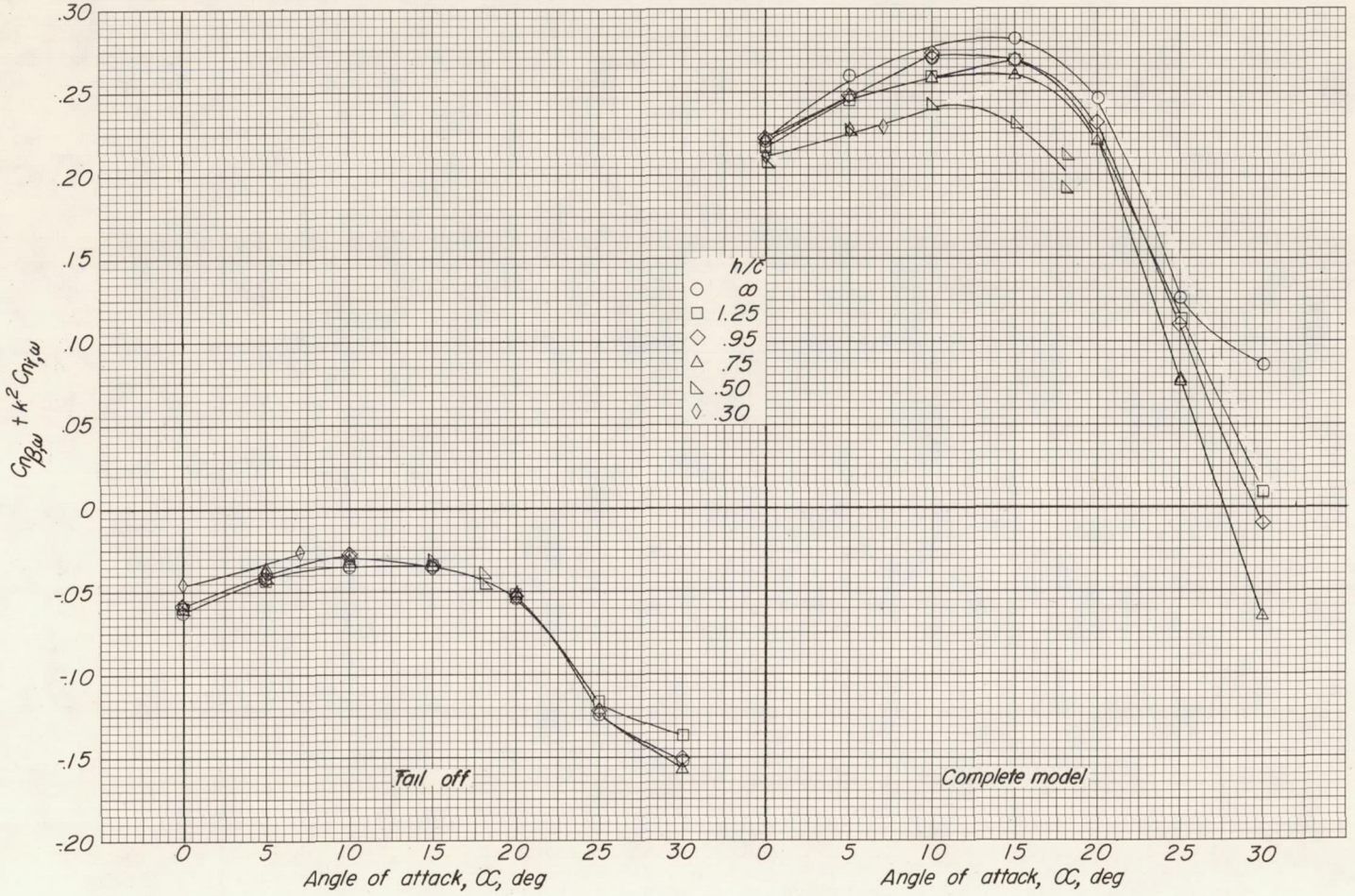

(d) Variation of $C_{n_{\beta,\omega}} + k^2 C_{n_{\dot{r},\omega}}$ with angle of attack for the model with split flaps.

Figure 4.- Concluded.

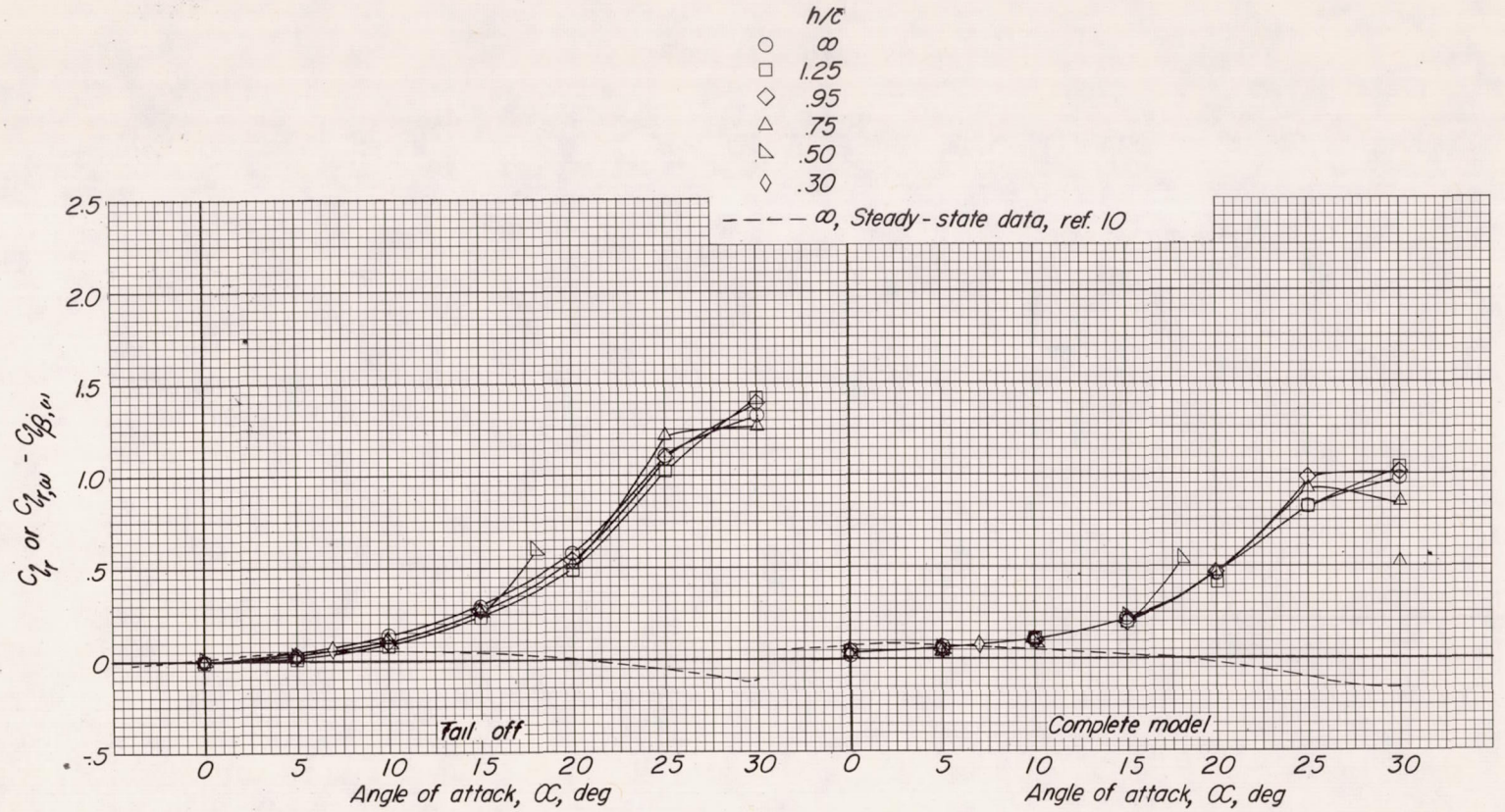

(a) Variation of C_{l_r} and $C_{l_{r,\omega}} - C_{l_{\dot{\beta},\omega}}$ with angle of attack for the model without split flaps.

Figure 5.- Effect of ground on the out-of-phase lateral oscillatory stability derivatives of a 60° delta-wing model with and without split flaps.

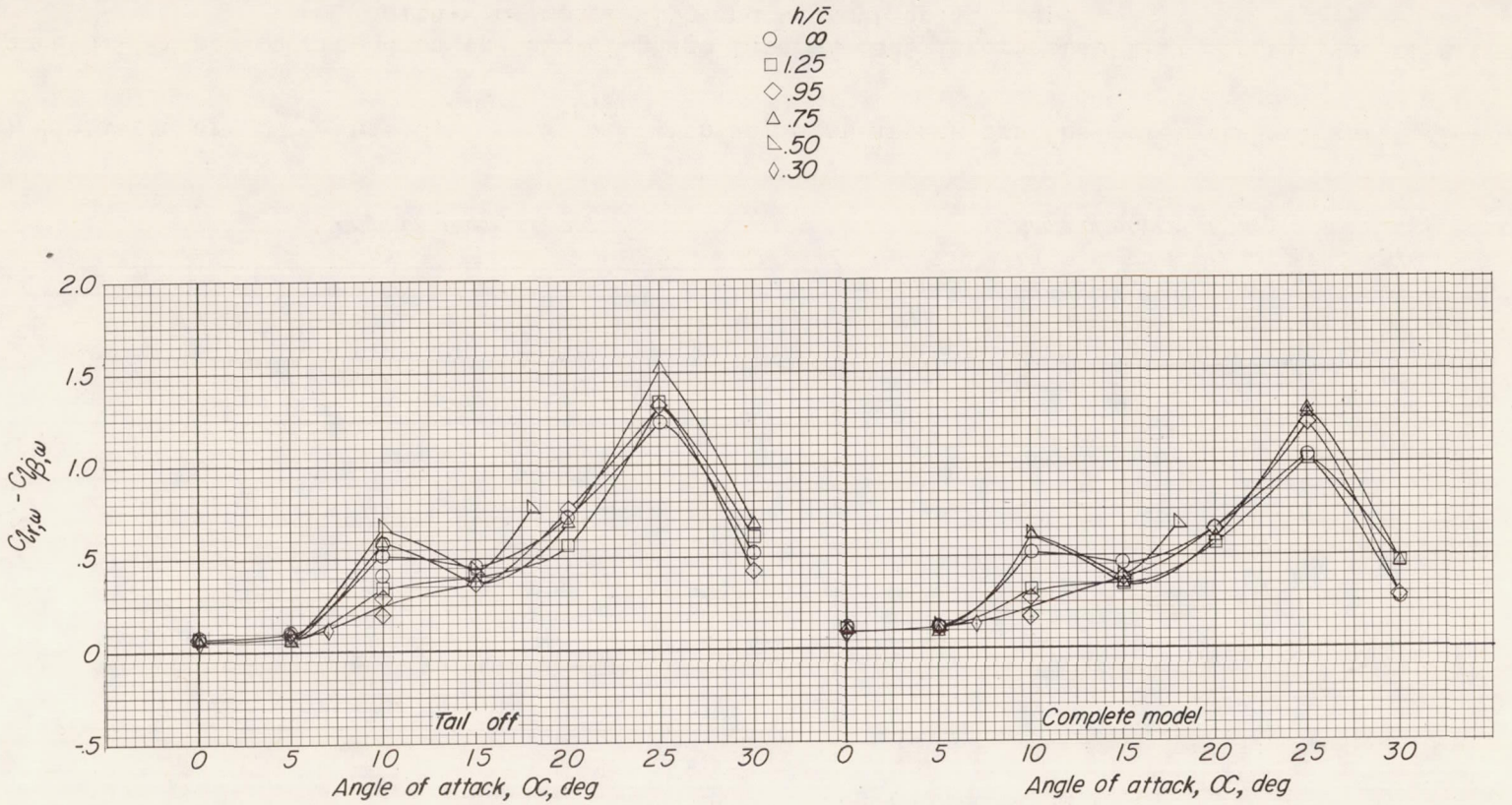

(b) Variation of $C_{l_{r,\omega}} - C_{l_{\dot{\beta},\omega}}$ with angle of attack for the model with split flaps.

Figure 5.- Continued.

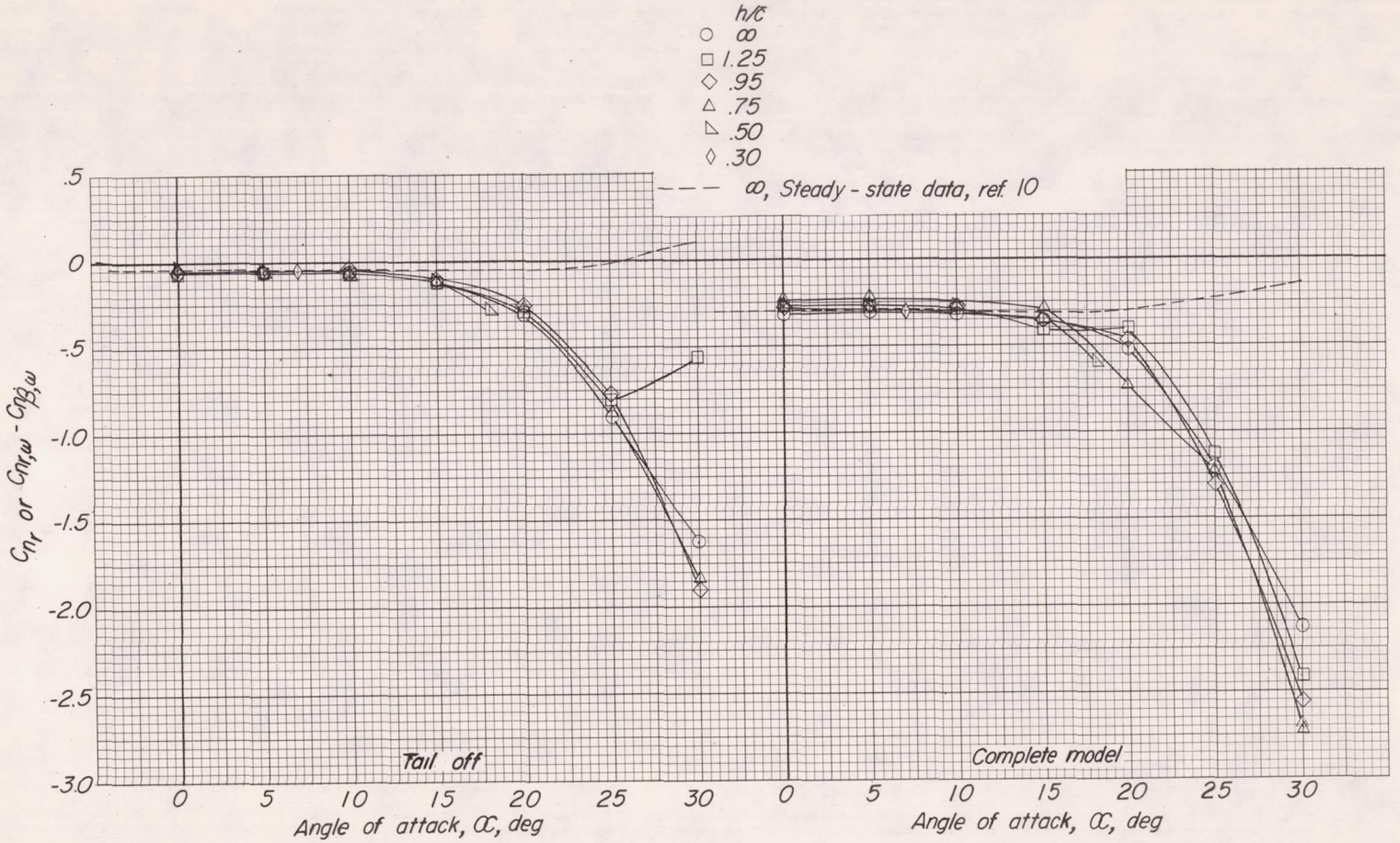

(c) Variation of C_{n_r} and $C_{n_{r,\omega}} - C_{n_{\dot{\beta},\omega}}$ with angle of attack for the model without split flaps.

Figure 5.- Continued.

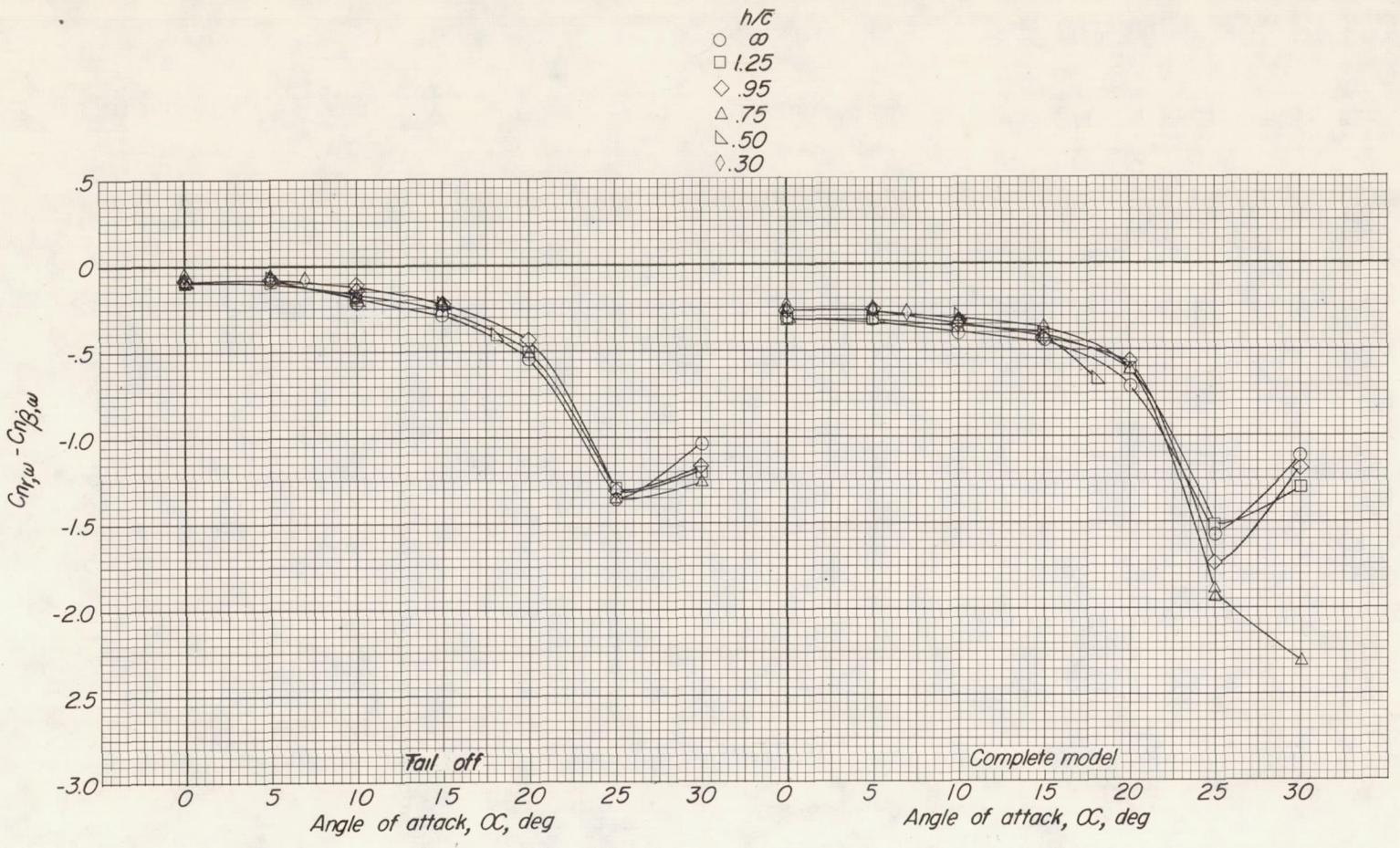

(d) Variation of $C_{n_{r,\omega}} - C_{n_{\dot{\beta},\omega}}$ with angle of attack for the model with split flaps.

Figure 5.- Concluded.

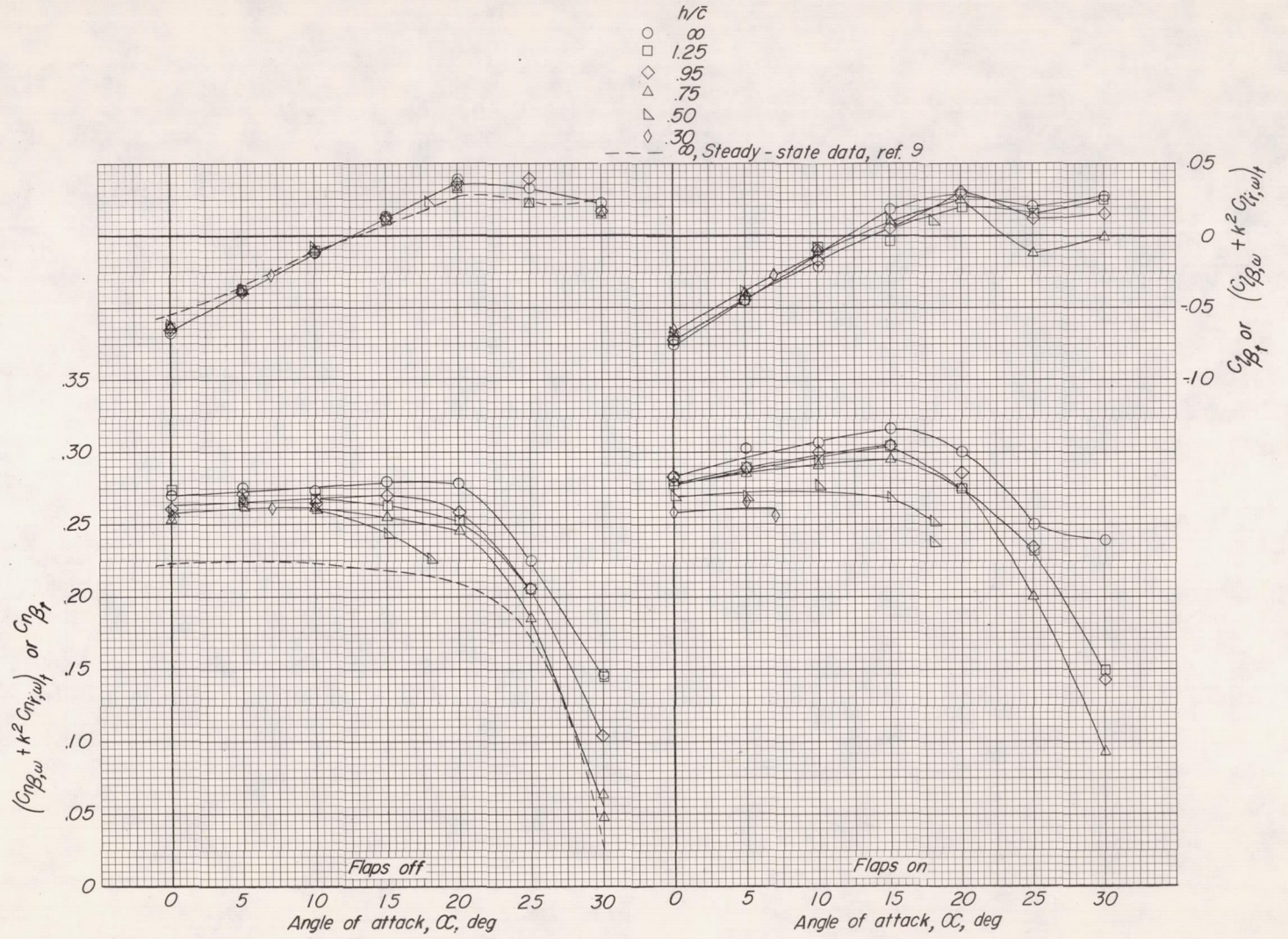

Figure 6.- Effect of ground on the tail contribution to the in-phase lateral oscillatory derivatives of a 60° delta-wing model with and without split flaps.

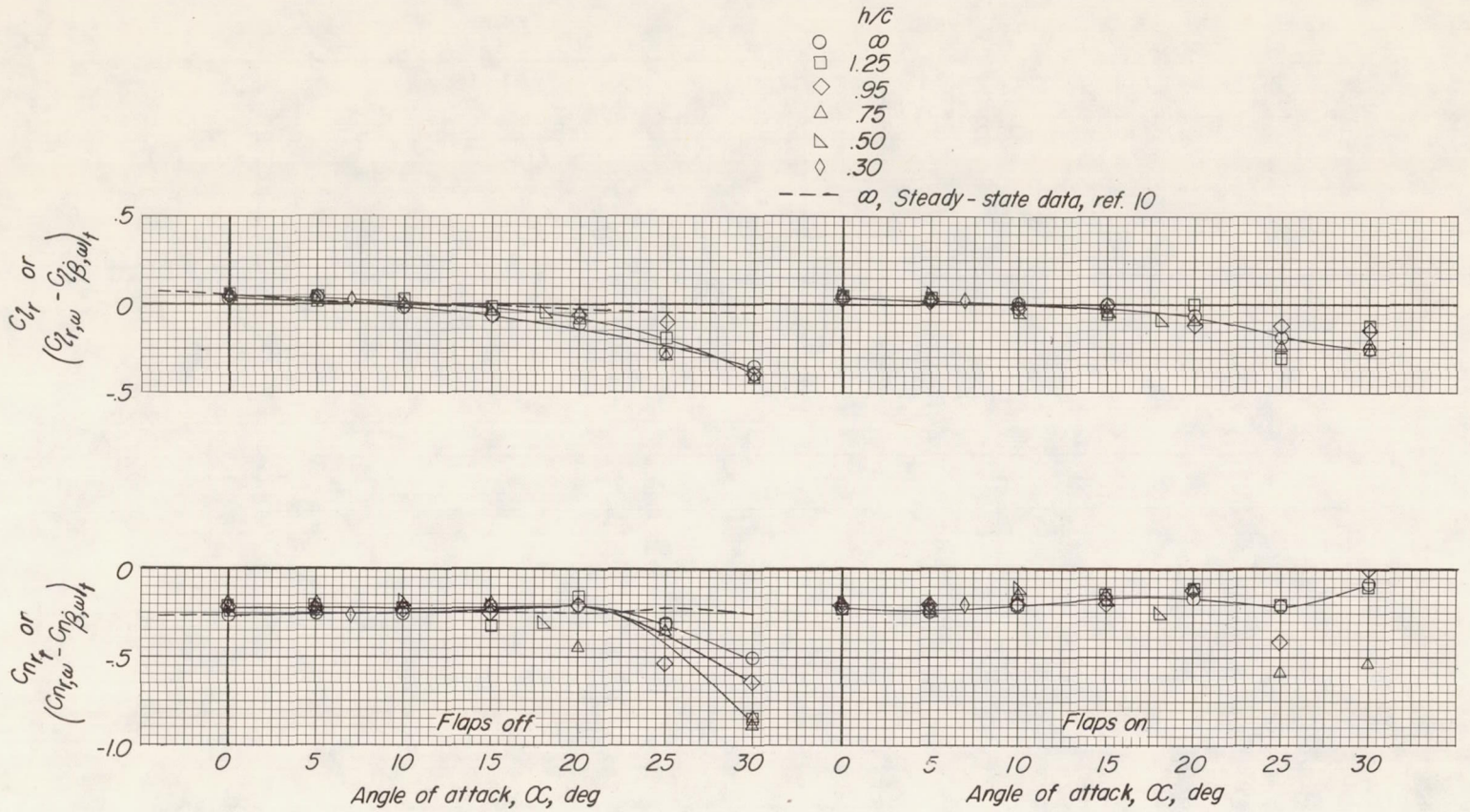

Figure 7.- Effect of ground on the tail contribution to the out-of-phase lateral oscillatory derivatives of a 60° delta-wing model with and without split flaps.

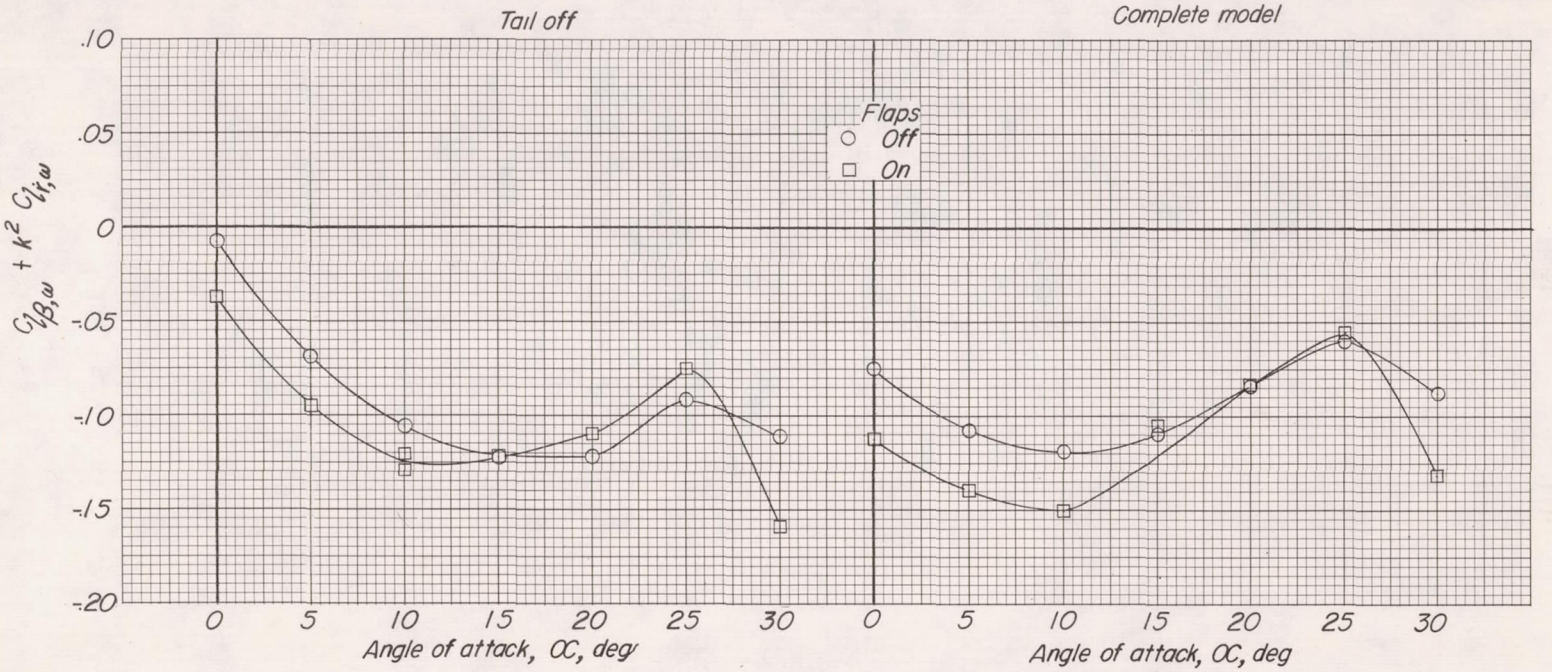

(a) Variation of $C_{l_{\beta,\omega}} + k^2 C_{l_{\dot{r},\omega}}$ with angle of attack.

Figure 8.- Effect of split flaps on the in-phase lateral oscillatory stability derivatives of a 60° delta-wing model with and without a vertical tail. $h/\bar{c} = \infty$.

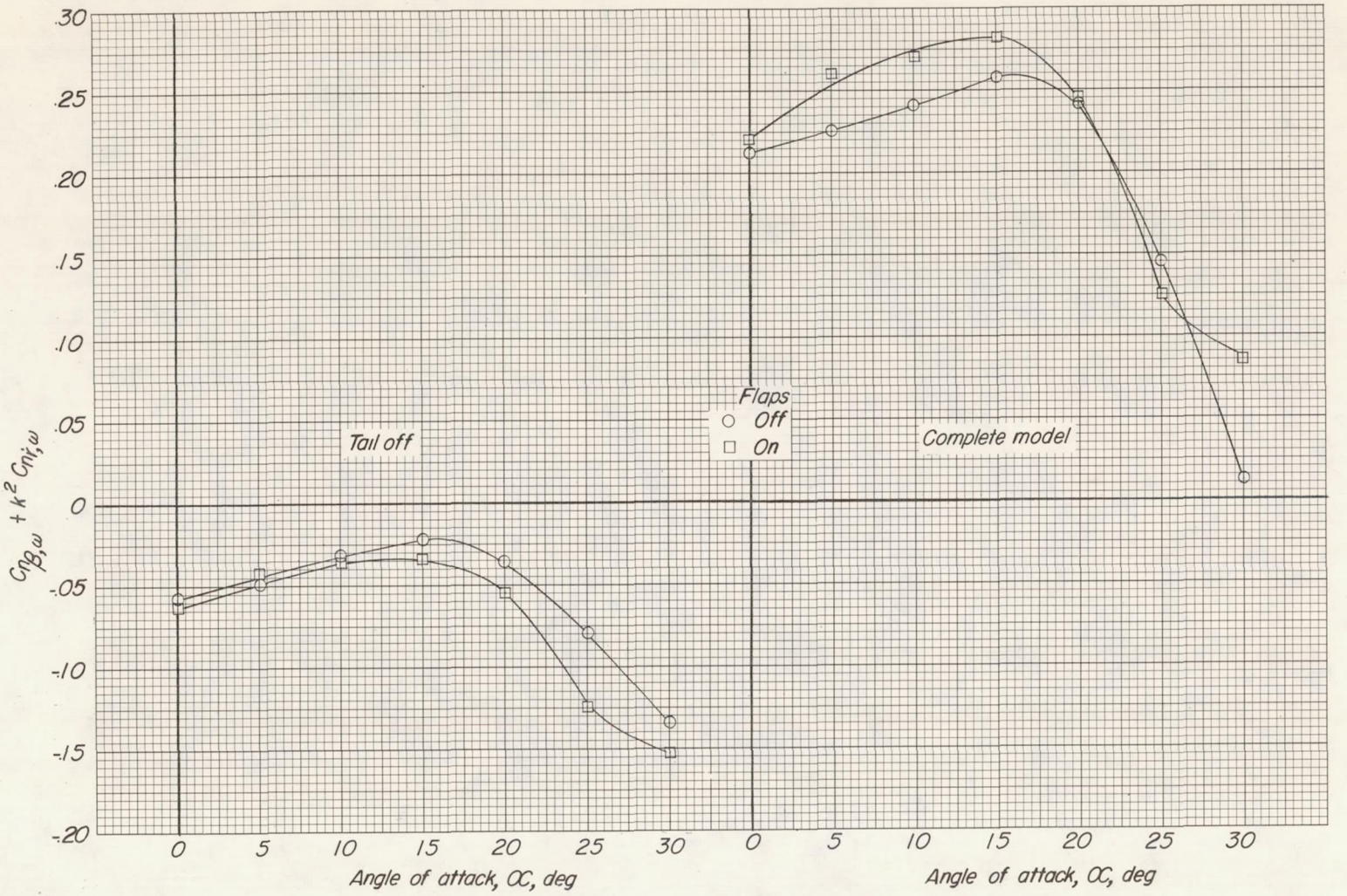

(b) Variation of $C_{n_{\beta,\omega}} + k^2 C_{n_{\dot{r},\omega}}$ with angle of attack.

Figure 8.- Concluded.

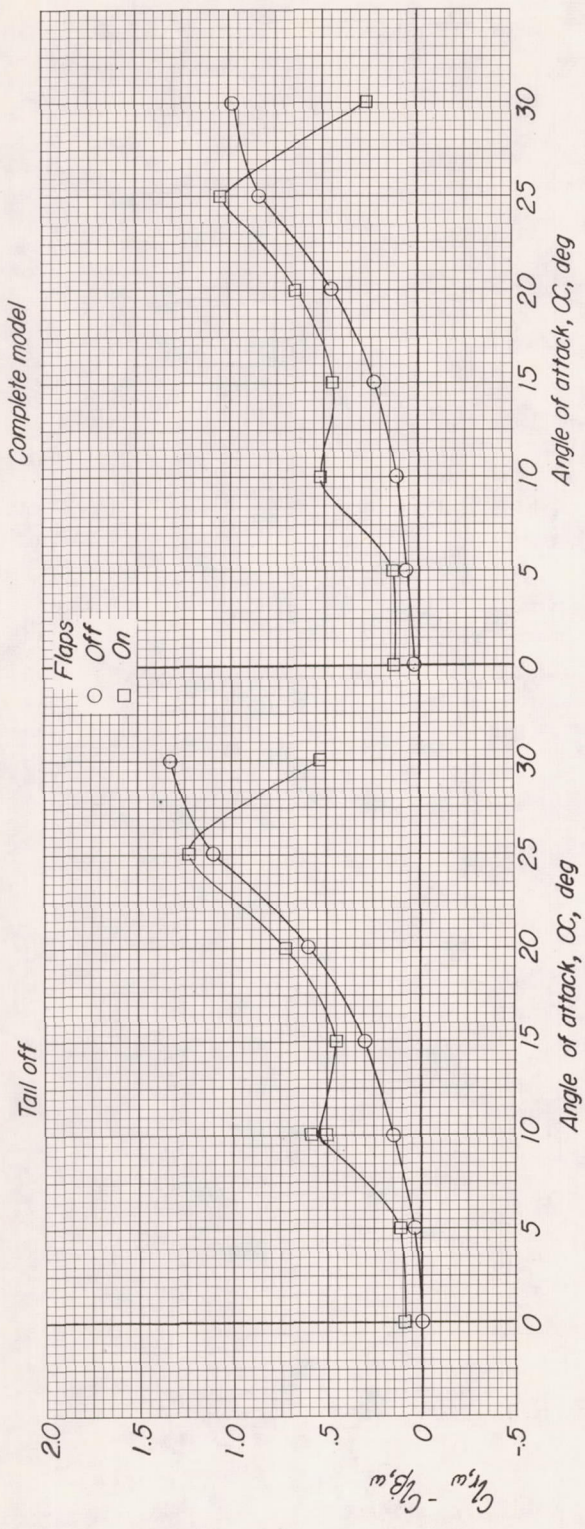

(a) Variation of $C_{l_r,\omega} - C_{l_{\dot{\beta}},\omega}$ with angle of attack.

Figure 9.- Effect of split flaps on the out-of-phase lateral oscillatory stability derivatives of a 60° delta-wing model with and without a vertical tail. $h/\bar{c} = \infty$.

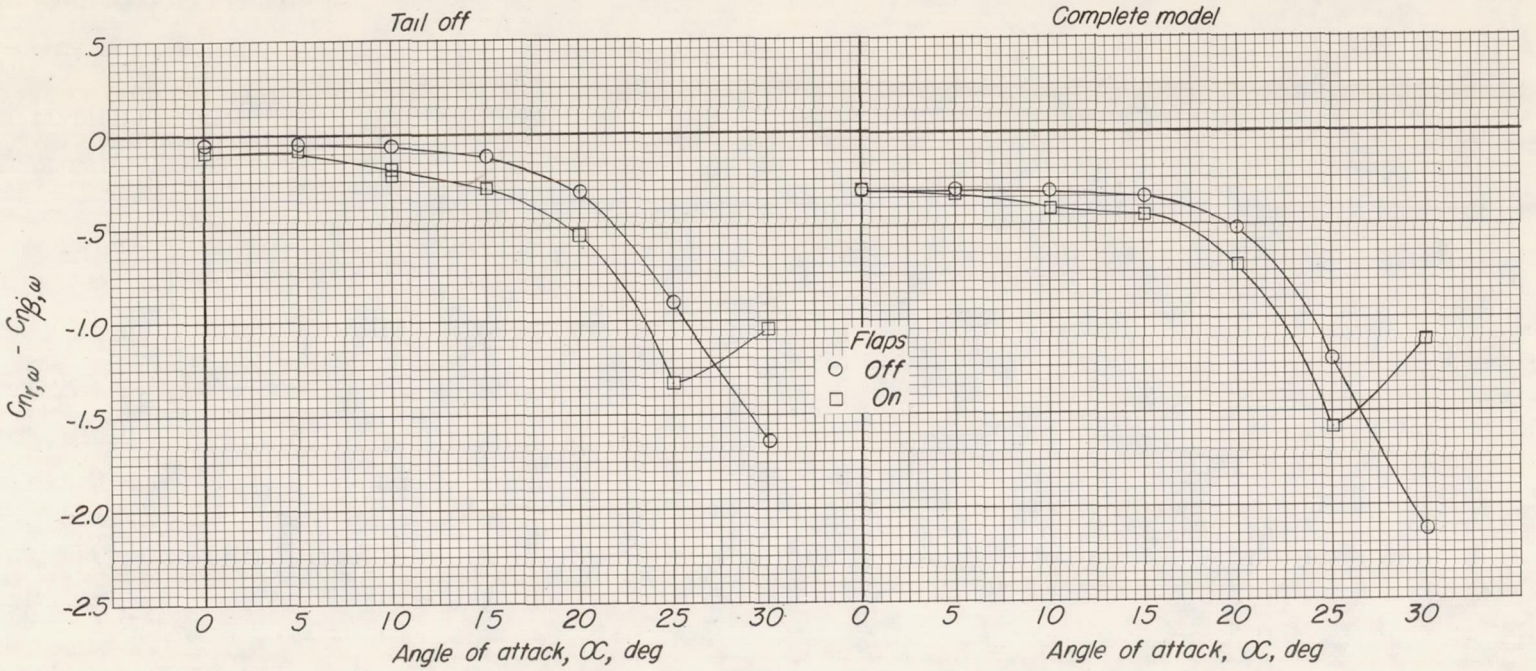

(b) Variation of $C_{n_{r,\omega}} - C_{n_{\dot{\beta},\omega}}$ with angle of attack.

Figure 9.- Concluded.

NACA - Langley Field, Va.